Protein Engineering, Design & Selection vol. 25 no. 11 pp. 725–731, 2012
Published online October 16, 2012 doi:10.1093/protein/gzs071

High-throughput screening system based on phenolics-responsive transcription activator for directed evolution of organophosphate-degrading enzymes

Young-Su Jeong[1†], Su-Lim Choi[2†], Hyun-Ho Kyeong[1], Jin-Hyun Kim[1], Eui-Joong Kim[3], Jae-Gu Pan[2], Eugene Rha[2], Jae Jun Song[2], Seung-Goo Lee[2,5] and Hak-Sung Kim[1,4,5]

[1]Department of Biological Sciences, Korea Advanced Institute of Science and Technology (KAIST), 291 Daehak-ro, Yuseong-gu, Daejeon 305-701, Korea, [2]Korea Research Institute of Biosciences and Biotechnology, Daejeon 305-806, Korea, [3]Genofocus, Inc., Daejeon 305-500, Republic of Korea and [4]Graduate School of Nanoscience and Nanotechnology (WCU), Korea Advanced Institute of Science and Technology (KAIST), 291 Daehak-ro, Yuseong-gu, Daejeon 305-701, Korea

[5]To whom correspondence should be addressed. hskim76@kaist.ac.kr (H.-S.K.); sglee@kribb.re.kr (S.-G.L.)

Received May 25, 2012; revised August 28, 2012; accepted September 5, 2012

Edited by Gideon Schreiber

Synthetic organophosphates (OPs) have been used as nerve agents and pesticides due to their extreme toxicity and have caused serious environmental and human health problems. Hence, effective methods for detoxification and decontamination of OPs are of great significance. Here we constructed and used a high-throughput screening (HTS) system that was based on phenolics-responsive transcription activator for directed evolution of OP-degrading enzymes. In the screening system, phenolic compounds produced from substrates by OP-degrading enzymes bind a constitutively expressed transcription factor DmpR, initiating the expression of enhanced green fluorescent protein located at the downstream of the DmpR promoter. Fluorescence intensities of host cells are proportional to the levels of phenolic compounds, enabling the screening of OP-degrading enzymes with high catalytic activities by fluorescence-activated cell sorting. Methyl parathion hydrolase from *Pseudomonas* sp. WBC-3 and *p*-nitrophenyl diphenylphosphate were used as a model enzyme and an analogue of G-type nerve agents, respectively. The utility of the screening system was demonstrated by generating a triple mutant with a 100-fold higher k_{cat}/K_m than the wild-type enzyme after three rounds of directed evolution. The contributions of individual mutations to the catalytic efficiency were elucidated by mutational and structural analyses. The DmpR-based screening system is expected to be widely used for developing OP-degrading enzymes with greater potential.

Keywords: directed evolution/high-throughput screening/organophosphate-degrading enzymes/transcription activator

Introduction

More than 200 organophosphates (OPs) are currently used as pesticides (Murphy, 1986), and OP nerve agents have been stockpiled as chemical warfare agents (CWAs) including tabun (GA), sarin (GB), soman (GD), GF and VX (Singh and Walker, 2006). Widespread use and reserves of these OPs have raised serious issues with regard to the environment and human health because of their inherent toxicity caused by inhibition of acetyl cholinesterase (Murphy, 1986; Briseño-Roa *et al*., 2006). Much effort has been directed toward the development of effective methods for decontamination and detoxification of OPs. Bleach treatment, alkaline hydrolysis and incineration are the major methods, but they require harsh conditions and discharge toxic byproducts. Hence, the development of efficient and environmentally benign methods would be of great significance.

The use of OP-degrading enzymes has attracted much attention, and diverse enzymes have been identified for such applications. Typical enzymes include phosphotriesterase (PTE) from *Pseudomonas diminuta* and *Flavobacterium* sp. (Mulbry *et al*., 1986) and organophosphorus acid anhydrolase (OPAA) from *Alteromonas* sp. (DeFrank and Cheng, 1991; Cheng *et al*., 1996). PTE shows substrate specificity for a broad range of OP pesticides including paraoxon, but has a low hydrolytic activity for OP nerve agents (Di Sioudi *et al*., 1999). Soluble expression of PTE in bacteria was difficult (Omburo *et al*., 1992; Shimazu *et al*., 2001), but it was significantly increased by mutations and use of molecular chaperons (Tokuriki and Tawfik, 2009). OPAA was reported to hydrolyze G-type nerve agents such as sarin and soman, but displaying no activity toward V-type nerve agents such as VX (Vyas *et al*., 2010). Methyl parathion hydrolase (MPH) from *Pseudomonas* sp. WBC-3 was shown to hydrolyze methyl parathion and other OPs, exhibiting different substrate specificity from PTE (Chen *et al*., 2002; Dong *et al*., 2005). Although MPH offers an advantage over other enzymes due to its high level of soluble expression in bacteria, it has a low catalytic activity toward OPs (Yang *et al*., 2008). To develop the enzymes for efficient detoxification, molecular evolution and isolation of enzymes with desired properties have been the primary approaches, which necessitate a high-throughput screening (HTS) system. Several screening methods based on agar plate and *in-vitro* compartmentalization were developed (Cho *et al*., 2002; Griffiths and Tawfik, 2003; Yang *et al*., 2003), but they have some drawbacks such as low-throughput screening, excess use of harmful analogues and difficulty in synthesizing fluorogenic substrates.

Here we present the construction and use of an HTS system based on phenolics-responsive transcription activator for directed evolution of OP-degrading enzymes. The

[†]Equally contributed to this work.

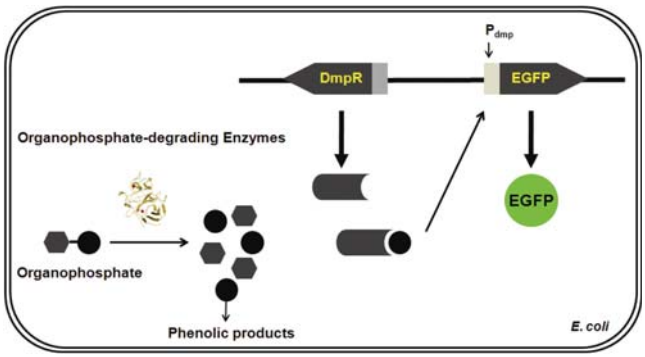

Fig. 1. Schematic of an HTS system based on phenolics-responsive transcription activator. The screening system is composed of a transcription activator DmpR, promoter P_{dmp} and EGFP which is located at the downstream of the P_{dmp} and used as a reporter. Phenolic compounds produced from OPs by OP-hydrolyzing enzymes bind a constitutively expressed transcription activator DmpR. The resulting DmpR complex activates the promoter P_{dmp}, initiating the expression of EGFP.

screening system was composed of the transcription factor DmpR, which is activated by phenolic compounds (Shingler and Moore, 1994; Pavel *et al*., 1994), the promoter P_{dmp} and enhanced green fluorescent protein (EGFP) (Fig. 1). Phenolic compounds produced from OPs by OP-degrading enzymes bind a constitutively expressed DmpR, initiating the expression of EGFP. Fluorescence intensities of host cells are proportional to the levels of phenolic compounds, and the cells expressing OP-degrading enzymes with high catalytic activities can be screened by fluorescence-activated cell sorting (FACS). MPH from *Pseudomonas* sp. WBC-3 was used as a model enzyme, and *p*-nitrophenyl diphenylphosphate (pNDP), which is a synthetic analogue of G-type nerve agents (Ibrahim and Ramadan, 2010; Menger and Tsuno, 1989), was employed as a typical OP. We demonstrated the utility of the screening system by generating a triple mutant with a 100-fold higher k_{cat}/K_m than the wild type by directed evolution. Mutational and structural analyses were conducted to elucidate the effect of individual mutations on the catalytic efficiency.

Materials and methods

Reagents

All OP pesticides including O,O-dimethyl O-(2-chloro-4-nitrophenyl)phosphorothioate (dicapthon), O,O-dimethyl O-(*p*-(dimethylsulfamoyl)phenyl) phosphorothioate (famphur), O,O-diethyl O-4-methylsulfinylphenyl phosphorothioate (fensulfothion), diethyl 4-nitrophenyl phosphate (paraoxon), O-4-cyanophenyl O,O-dimethyl phosphorothioate (cyanophos), O,O-diethyl O-3,5,6-trichloropyridin-2-yl phosphorothioate (chlorpyrifos), O,O-dimethyl O-(3,5,6-trichloro-2-pyridyl) phosophorothioate (chlorpyrifos-methyl), and O,O-dimethyl O-*p*-nitrophenyl phosphorothioate (methyl parathion) were purchased from Sigma-Aldrich. Chemical structures of OPs are shown in Supplementary Fig. S2. pNDP was supplied by the Agency for Defense Development (ADD, Korea), and used as an analogue of the G-type CWAs (Ibrahim and Ramadan, 2010; Menger and Tsuno, 1989). Carbenicillin and kanamycin were obtained from Sigma-Aldrich. Luria–Bertani (LB) agar and broth were purchased from Duchefa Biochemie. Restriction enzymes, T4 DNA ligase, thermophilic polymerases and other polymerase chain reaction (PCR) reagents were purchased from TaKaRa Bio. The plasmid pTrc99A and pPROLarA.122 were obtained from Amersham Pharmacia Biotech and Clontech, respectively. The pMAL-c2x plasmid was obtained from New England Biolabs. Oligonucleotides were synthesized by Bioneer. All other reagents were purchased from commercial sources and were of analytic grade.

Construction of a screening system

We designed a screening system composed of the transcription activator DmpR, promoter P_{dmp} and EGFP. The dmp operon encodes enzymes involved in the catabolism of phenols in the *Pseudomonas* sp. strain CF600 (Shingler and Moore, 1994). DmpR was shown to be a transcriptional activator of the NtrC family, initiating the transcription of the dmp operon in response to phenolic compounds. To construct the screening plasmid pUEGFP-DmpR, the promoter P_{dmp} was amplified from *Pseudomons* sp. strain CF600 and fused to the EGFP gene by overlap PCR. In this study, the DmpR variant harboring the E135K mutation was used because this DmpR variant was shown to respond more sensitively to *para*-substituted phenolic compounds as well as other phenolics (Pavel *et al*., 1994). The resulting DmpR variant was cloned under the constitutive expression promoter, P_{hce}, originated from *Geobacillus toebii* (Poo *et al*., 2002). Thus, the plasmid pUEGFP-DmpR contained a constitutively expressed transcription activator DmpR, promoter P_{dmp} and EGFP which was located at the downstream of P_{dmp}. The plasmid pPROTrc, which was used as a library plasmid, was constructed by replacing the $P_{lac/ara-1}$-derived promoter with P_{trc} originating from pTrc99A for isopropyl-β-D-thiogalactoside (IPTG) induction. For replacement, a derivative of pTrc99A harboring a 300 bp ApaLI–HindIII DNA fragment was subcloned into the corresponding sites of pPROLarA.122.

Construction of a mutant library

Escherichia coli competent cells harboring the screening plasmid, pUEGFP-DmpR, were prepared. *E.coli* XL1-Blue, which was used as the host cell for generating a library, was constructed by insertion of the screening plasmid pUEGFP-DmpR and the library plasmid pPROTrc. MPH originated from *Pseudomonas* sp. WBC-3 was generously provided by Dr Zang (Dong *et al*., 2005). A random library was constructed for directed evolution of MPH by error-prone PCR at a mutation frequency of two to three substitutions per whole amino acids in the enzyme. The PCR mixture contained KCl (50 mM), $MgCl_2$ (7 mM), $MnCl_2$ (0.1 mM), dGTP (0.2 mM), dATP (0.2 mM), dCTP (1 mM), dTTP (1 mM), template plasmid (about 100 pg in 50 μl reaction mixture), primers (each 0.5 mM) and Taq DNA polymerase (2.5 unit per 50 μl reaction mixture) in Tris-HCl (10 mM, pH 8.3). The primers used were N-(5′-TGGAATTCC ACCATCACCATC-3′) and C-(5′-CCAAGCTTTCACTTGG GGTTG-3′). The reaction was performed at 94°C for 5 min, followed by 35 cycles at 94°C for 30 s, 55°C for 1 min, 72°C for 30 s and finally at 72°C for 5 min. The error-prone PCR products were cloned into the pPROTrc plasmid using the restriction enzymes EcoRI, HindIII and T4 DNA ligase. The ligated plasmids were transformed into the *E.coli* XL1-Blue competent cells harboring the plasmid pUEGFP-DmpR by heat shock at 42°C for 90 s. Transformants were plated on LB agar plates containing carbenicillin (100 μg ml^{-1}) and kanamycin (50 μg ml^{-1}), which was followed by overnight

incubation at 37°C. The average size of the library was about 2.2×10^6. The library was collected using scrapers, washed twice and re-suspended in LB media having carbenicillin (100 μg ml^{-1}), kanamycin (50 μg ml^{-1}) and 20% glycerol. The resuspended library in LB-containing glycerol was stored in a deep freezer at −72°C. Libraries of second and third rounds were constructed with the most improved mutant in the first and second library using the same error-prone PCR method, and their sizes were estimated to be 5.5×10^7 and 1.2×10^6, respectively. Mutation frequency of the libraries was about two to three substitutions per whole amino acids in the enzyme. Nucleotide sequences of selected transformants from the libraries were determined by Macrogen (Seoul, Korea).

Screening of MPH variants by flow cytometry

A mutant library was inoculated in 5 ml of LB medium containing carbenicillin (100 μg ml^{-1}) and kanamycin (50 μg ml^{-1}), which was followed by overnight cultivation at 37°C on an orbital shaking at 180 rpm. The grown cells ware re-inoculated in 5 ml of LB medium supplemented with carbenicillin (100 μg ml^{-1}) and kanamycin (50 μg ml^{-1}) at 37°C. When the optical density reached $OD_{600} = 0.4$, IPTG was added at final of concentration of 1.0 mM, and the cells were further grown at 30°C for 6–8 h. Grown cells were harvested, washed and re-suspended with phosphate-buffered saline (PBS) buffer followed by the addition of pNDP. After 4 h of incubation with a substrate, the cells showing higher fluorescence intensities were screened using a FACSAria™ Automated Flow Cytometer Sorter (BD Biosciences) and full HTS system composed of JANUS™ Automated Liquid Handling (PerkinElmer), CRS F3 Articulated robot (Thermo Electron Corp.), LiCONiC Automated Incubator and Victor III Multilabel Microplate Reader (PerkinElmer) in KRIBB Jeonbuk Branch (Jeongeup, Korea). A typical procedure for sorting and analyzing the cells expressing the MPH variants using a flow cytometry after reaction with pNDP is shown in Supplementary Fig. S3. The cells with a normal size were marked as blue spots in the P3 region (Supplementary Fig. S3A) and subjected to a single-cell sorting. Eventually, cells in the P5 region, the top 1.5% of the cells in the P3 region showing high EGFP signals, were sorted into 96-well plates containing 200 μl of LB medium with kanamycin (50 μg ml^{-1}) in each well using FACSAria™ Automated Flow Cytometer Sorter (Supplementary Fig. S3B). All 96 plates were transferred to a full HTS system, and cells were grown to the stationary phase at 37°C for 2 days at a shaking speed of 300 rpm in a LiCONiC Automated Incubator. Grown cells in each 96-well plates were inoculated into new 96-well plates containing 200 μl of LB medium with kanamycin (50 μg ml^{-1}) using JANUS™ Automated Liquid Handling and incubated for 6 h at 300 rpm. Following the addition of IPTG to a final concentration of 1 mM, the cells were grown overnight at 30°C and a shaking speed of 300 rpm. The substrate pNDP was added to each well at a final concentration of 100 μM. Changes in the absorbance at 405 nm were monitored using a Victor III plate-reader, and cells showing the highest signals were isolated. Variants in the libraries of second and third rounds were also screened by the same procedure.

Expression, purification and characterization of evolved variants

The selected mutants were amplified using a PrimeSTAR DNA polymerase and the primers previously used. The F196A and L273A mutants were constructed using the following primers: N-(5′-GGCGCCTTTGAAGGCGCCTTT GCTCTC-3′) and C-(5′-GAGAGCAAAGGCGCCTTCAAA GGCGCC-3′) for the F196A mutant, and N-(5′- GCTGT CGCTGTCGGCCTGGGTCGTGAC-3′) and C-(5′- GTCAC GACCCAGGCCGACAGCGACAGC-3′) for the L273A mutant. The PCR mixture contained 50 mM KCl, 5 mM $MgCl_2$, 2.5 mM dNTP, template plasmid (about 100 pg in 50 μl reaction mixture), 0.5 mM primers and Taq DNA polymerase (2.5 unit per 50 μl reaction mixture) in 10 mM Tris-HCl (pH 8.3). The reaction was performed at 95°C for 10 min, followed by 30 cycles at 95°C for 1 min, 55°C for 1 min, 72°C for 1 min and 72°C for 10 min. The PCR products were introduced into the expression vector pMAL-c2x using the restriction enzyme EcoRI and HindIII and T4 DNA ligase, and transformed into *E.coli* XL1-Blue. Nucleotide sequences of the mutants were determined by Macrogen (Seoul, Korea). The mutants were grown at 37°C in LB medium containing carbenicillin (100 μg ml^{-1}) and $ZnCl_2$ (0.2 mM). When the OD_{600} reached 0.4, IPTG was added to a final concentration of 0.5 mM, which was followed by further incubation at 37°C for 6 h. The MBP-fused proteins were purified using a MBP Excellose SPIN Kit (TaKaRa Bio) according to the manufacturer's instructions. The concentration of purified enzyme was determined by Bradford assays. The enzyme activity was measured by measuring the absorbance changes at 405 nm. One milliliter of the reaction mixture contained 50 mM Tris-HCl (pH 7.0), 100 mM NaCl, 0.2 mM $ZnCl_2$, 0.1% Triton X-100, purified enzyme (100 μl of 0.2 mg ml^{-1}) and pNDP (10 μl of 3∼10 mM) dissolved in DMSO. The initial reaction rates were determined at different substrate concentrations, and the K_m and k_{cat} values were obtained from the Lineweaver-Burk plots. To verify the sensitivity of the genetic circuit-based screening system, the cells expressing the wild-type and mutant enzymes isolated at each round of directed evolution were cultivated in 5 ml of LB medium and induced by IPTG at $OD_{600} = 0.4$. Cells were further grown at 30°C for 6–8 h. Grown cells were harvested, washed and re-suspended with PBS buffer followed by the addition of the substrate pNDP. After incubation with the substrate for 15 min, about 10 000 cells expressing respective enzymes were analyzed using an FACS.

Structural analysis of mutant enzymes

For modeling the enzyme structures, the SWISS-MODEL homology modeling server was used (Guex and Peitsch, 1997; Schwede *et al*., 2003; Arnold *et al*., 2006). The structure of the wild-type MPH (PDB:1P9E) was used as a reference. The protein surfaces were calculated and rendered using PyMOL (DeLano, 2002). Molecular dynamics simulation and root mean square fluctuation (RMSF) analysis were performed using the GROMACS package version 4.5.3 with the GROMOS53a6 force field (Oostenbrink *et al*., 2004; Van Der Spoel *et al*., 2005; Hess *et al*., 2008). Mutant structures were generated using SCWRL4 based on the wild-type MPH

(Krivov *et al.*, 2009). An ordinary protocol was employed and consisted of steepest gradient energy minimization by molecular dynamics simulation in a 1-ns equilibration phase and a 3-ns production phase. Temperature was maintained at 298 K using a Berendsen weak-coupling thermostat and all bonds were treated as constraints in the LINCS algorithm (Berendsen *et al.*, 1981, 1984). Particle mesh Ewald summation was used to treat long-range electrostatics. Enzymes were solvated in SPC water in cubic boxes with a spacing of 10 Å. The regular leap-frog MD integrator simulated physics at a time step of 2 fs. Coordinates were saved every picosecond, and the trajectory from the 3000-ps production phase was used for RMSF analysis. RMSF was computed from a set of uniformly aligned coordinates, and proper alignment was critical for obtaining meaningful results. In order to better differentiate flexible and rigid parts of the enzyme, a two-step superposition procedure was used. In the first step, all backbone atoms of the wild-type MPH and mutant were used for alignment and preliminary RMSF values were calculated. These values were used to sort out the most stable half among the backbone atoms, which were used as the basis of the second alignment. From the second aligned trajectory, final RMSF values were calculated. All alignments were performed using the trjconv program of the GROMACS package.

Results and discussion

Design and construction of an HTS system

For directed evolution of OP-degrading enzymes, we constructed a HTS system comprising phenolics-responsive transcription activator DmpR and EGFP (Fig. 1). Briefly, phenolic products released from OPs by OP-degrading enzymes bind the constitutively expressed transcription activator DmpR in *E.coli* host, inducing the expression of EGFP as a reporter protein. The fluorescence intensities of the host cells are dependent on the levels of phenolic compounds, and the cells expressing the enzymes with high catalytic activities can be screened by FACS. We first examined whether the constructed host cells display fluorescence signals in response to exogenously added *p*-nitrophenol, and observed significant signals within micro-molar range of *p*-nitrophenol (data not shown). We then tested pNDP which is a synthetic analogue of G-type nerve agents. In the case of pNDP, *p*-nitrophenol is produced by the action of MPH as depicted in Fig. 2A. XL1-Blue *E.coli* cells harboring the pPROTrc with wild-type MPH and the screening plasmid pUEGFP-DmpR were used as a positive control, whereas XL1-Blue cells containing the screening plasmid and pPROTrc without MPH were employed as a negative control (Supplementary Fig. S1). As shown in Fig. 2B, the positives cells exhibited higher

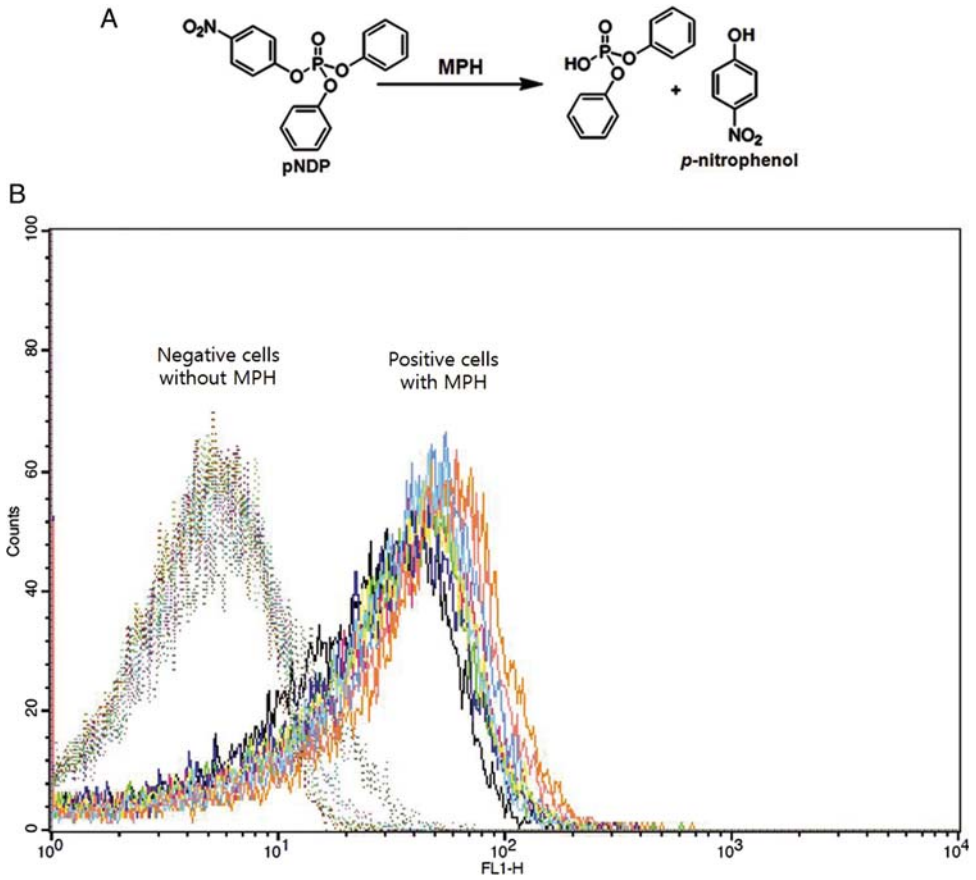

Fig. 2. Sorting and analysis of the cells displaying the fluorescence signals in response to OPs by flow cytometry. (**A**) Reaction scheme for hydrolysis of pNDP by MPH. (**B**) Analysis of the cells displaying the fluorescence signals for various OPs by flow cytometry. The cells harboring the screening plasmid pUEGFP-DmpR and MPH were incubated with 100 μM OPs, and analyzed by FACS. Each OP is represented by different color lines: apricot; pNDP, black; dicapthon, green; famphur, pink; fensulfothion, blue; paraoxon, orange; cyanophos, dark blue; chlorpyrifos, yellow; chlorpyrifos-methyl, azure; methyl parathion. Negative cells without MPH are indicated by the dotted lines, whereas positive cells containing MPH are marked by the solids line. About 10 000 cells were analyzed by flow cytometry. The *X*- and *Y*-axis show the fluorescence intensity and the cell counts, respectively.

fluorescence signals than the negative ones when incubated with 100 μM of pNDP. To check the generality of the screening system, we tested other OPs containing phenolic groups, and their chemical structures are shown in Supplementary Fig. S2. Following incubation with 100 μM of eachOP, the positive and negative cells were subjected to analysis by flow cytometry. As shown in Fig. 2B, the positive cells exhibited higher fluorescence signals than the negative ones in response to the tested OPs. More than 50% of widely used OP pesticides as well as many synthetic analogues of nerve agents such as soman and sarin contain phenolic groups, and these phenolic groups are released by the action of OP-degrading enzymes (Pope, 1999; Tsai *et al*., 2010). Because the use of real nerve agents is extremely dangerous and limited, such synthetic analogues have been employed for developing the enzymes against nerve agents (Tsai *et al*., 2010). Thus, our results support that the constructed screening system can find wide applications to the development of enzymes for diverse OPs.

A mutant library construction and screening of positive clones

Next, we tested if the screening system can be used for directed evolution of MPH. For this, a mutant library was constructed by introducing random mutations into the MPH gene using error-prone PCR, and an average mutation frequency was two to three substitutions in the amino acid sequence of MPH. The host cells expressing variants with higher catalytic activities are expected to display higher fluorescence signals than those expressing the starting enzyme because expression levels of EGFP become higher due to increased concentrations of phenolic compounds. For screening of improved mutants from the libraries, FACS sorting and full HTS were used. The MPH variants showing an increase in absorbance compared with the wild-type enzyme were selected, and the catalytic activity of the MPH variants was measured. As a result, the cells with high fluorescence signals were shown to express the MPH variants

Table I. Kinetic constants of the evolved enzymes and constructed single mutants

Round	Mutants	k_{cat} (s^{-1})	K_m (mM)	k_{cat}/K_m (M^{-1} s^{-1})	Fold increased
	wtMPH	0.55 ± 0.13	0.74 ± 0.13	7.40×10^2	1.0
1	Q81L	0.51 ± 0.12	0.35 ± 0.09	1.46×10^3	2.0
2	Q81L/F196A	25.65 ± 3.15	0.43 ± 0.07	6.01×10^4	81.3
3	Q81L/F196A/L273A	48.15 ± 10.94	0.65 ± 0.11	7.43×10^4	100.5
	F196A	43.04 ± 5.92	2.00 ± 0.12	2.16×10^4	29.2
	L273A	0.48 ± 0.06	0.24 ± 0.05	2.01×10^3	2.7

Each value represents mean and standard deviation in triplicate experiments.

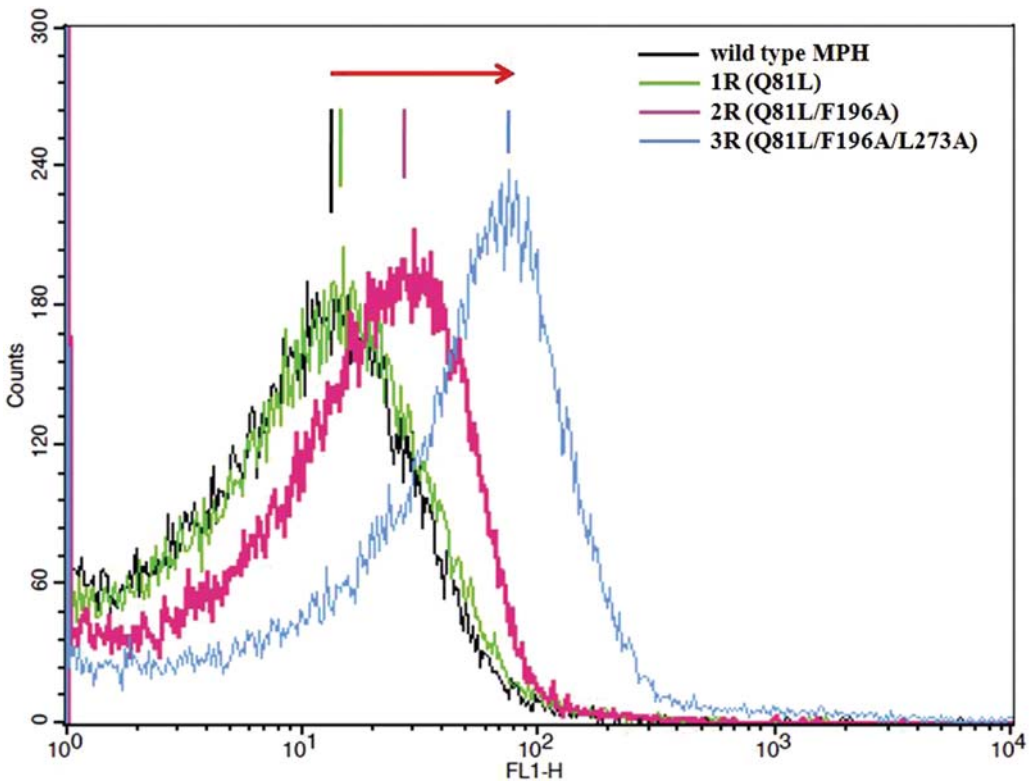

Fig. 3. Analysis of the cells expressing the enzymes with different catalytic efficiencies for pNDP by flow cytometry. Host cells expressing the wild-type and mutant enzymes isolated at each round of directed evolution were analyzed using FACS. The *X*- and *Y*-axis represent the fluorescence intensity and the cell counts, respectively.

with higher catalytic activities than the wild-type or parent MPH.

Directed evolution and mutational analysis

We conducted directed evolution of MPH using the constructed screening system. The MPH variants showing highest signals were selected at each round, and their kinetic constants were determined after purification (Table I). In the first round of directed evolution, we isolated three single mutants showing increased activities compared with the wild-type enzyme: E283A, S275C and Q81L. Of them, the Q81L exhibited a 2-fold higher k_{cat}/K_m value than the wild-type. At the second round of directed evolution, the double mutant (Q81L/F196A) was selected, showing a 81-fold higher catalytic efficiency than the wild-type enzyme. The third rounds of directed evolution generated a triple mutant (Q81L/F196A/L273A) showing a 100-fold enhanced k_{cat}/K_m compared with the wild-type MPH. Based on the amino acid changes in the evolved enzymes, beneficial mutations are likely to have accumulated as directed evolution proceeded, resulting in the mutant with a 100-fold increased k_{cat}/K_m. To verify the sensitivity of the developed screening system, we analyzed EGFP expression of cells expressing the wild-type and mutant enzymes isolated at each round of directed evolution after reaction with pNDP by flow cytometry. As a result, the fluorescence intensities of the cells were enhanced significantly with the increasing catalytic efficiency of the enzyme (Fig. 3), which confirms the sensitive and easy screening of the positive mutants in a high-throughput manner. This result indicates that the screening system can be effectively used for directed evolution of OP-degrading enzymes.

To assess the effect of individual mutations on the catalytic efficiency, we constructed the single mutants containing beneficial mutations found in the evolved enzymes by site-directed mutagenesis. Kinetic constants of the constructed mutants are shown in Table I. Notably, the k_{cat} value of the F196A mutant was 78-fold higher than the wild-type MPH and a 2.7-fold increase in K_m was observed, which resulted in a 29-fold increase in the k_{cat}/K_m value. These results clearly demonstrate that substitution of phenylalanine with alanine at position 196 significantly increased the catalytic efficiencies of the selected mutants (Q81L/F196A and Q81L/F196A/L273A). The L273A mutation led to a 3-fold decrease in the K_m value, whereas the k_{cat} value remained almost constant compared with the wild-type MPH, leading to 3-fold increase in the k_{cat}/K_m value. The Q81L mutation led to 2-fold decrease in the K_m value; however, the k_{cat} value was similar with the wild-type MPH. Based on the mutational analysis, it is clear that the F196A mutation

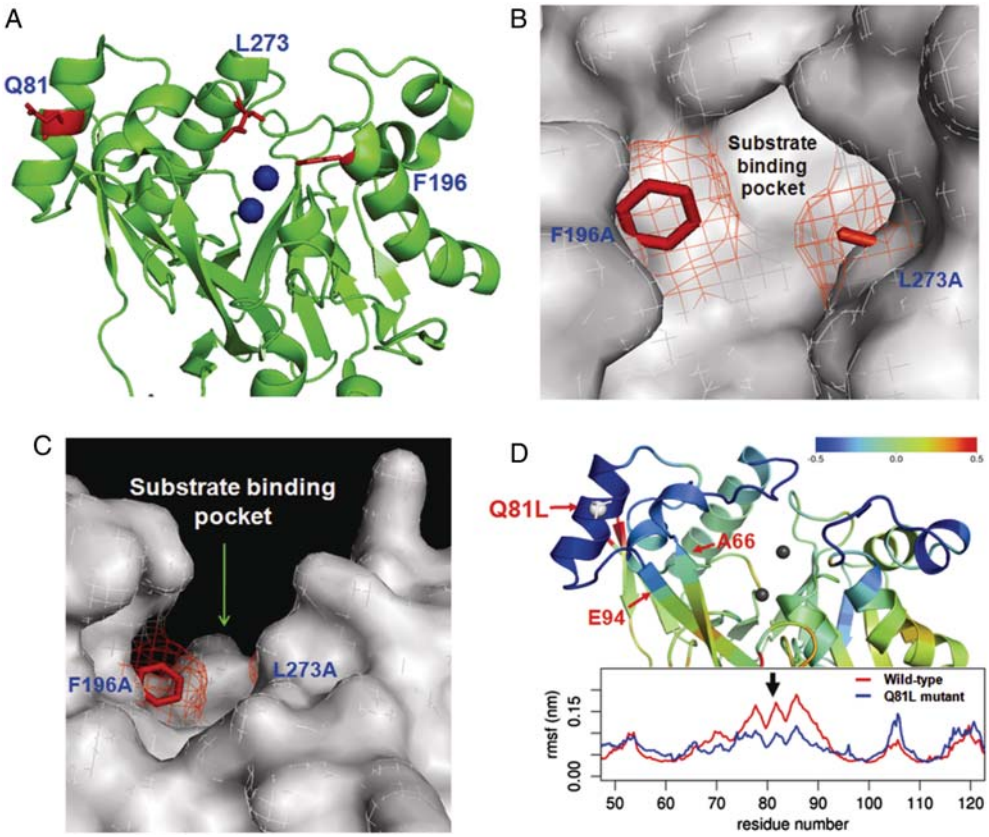

Fig. 4. Structural analysis of the mutations on the evolved MPH. (**A**) Mutated sites on the mutant selected at the third round of directed evolution. The structure of the wild-type MPH (PDB ID: 1P9E) was used as a reference. Q81 was located at a helix on the surface, whereas F196 and L273 were positioned in the substrate binding pocket. The blue-colored circles indicate zinc atoms at the active site. (**B**) Substrate binding pocket of the variant with the F196A and L273A mutations. For structural analysis of the substrate binding pocket between the wild-type MPH and the F196A/L273A mutant, homology modeling was carried out using the SWISS-MODEL. Red lines indicate the electron density of the wild-type enzyme, and the gray color represents the surface of the mutant. The protein surfaces were calculated and rendered using PyMOL. (**C**) Side view of the substrate binding pocket with the F196A and L273A mutations. Red lines represent the electron density of amino acid residues of the wild-type enzyme, and the gray color indicates the surface of the mutant. (**D**) RMSF analysis of the Q81L mutation. RMSF relative to the wild-type was shown in color, following the color band. Blue represents a decrease in RMSF, whereas red represents an increase. RMSF of both wild-type and the Q81L mutant were plotted against the residue number.

significantly contributes to the increase in the catalytic efficiencies of the evolved enzymes.

Structural analysis of mutations

Structural analysis was carried out to obtain better insight into the effect of these mutations (Q81L, F196A and L273A) on the catalytic efficiency. The three mutated sites on MPH are shown in Fig. 4A. The F196A and L273A mutations occurred at the substrate binding pocket of the enzyme. These mutations are likely to enlarge the substrate binding pocket when compared with the wild-type enzyme (Fig. 4B and C), which would increase the catalytic efficiency. The effect of the F196A mutation was found to be much higher than that of the L273 mutation (Table I). Based on this analysis, replacement of large amino acid residues with smaller sized one at the substrate binding pocket seemed to facilitate access of the substrate, resulting in a significant increase in the catalytic efficiency of the evolved enzymes. As for the Q81L mutation, a polar uncharged residue was replaced with a leucine at the surface of the enzyme, which led to a 2-fold increase in the catalytic efficiency of the mutant. To assess the contribution of this mutation to the catalytic efficiency, we compared the RMSF profile between the wild-type MPH and the Q81L mutant using molecular dynamics simulation (Fig. 4D). The RMSF has been widely used to measure the structural stability of proteins. The Q81 mutation at the surface resulted in a reduction in the fluctuation of the segment between A66 and E94, which constitutes part of the active site channel. Thus, stabilization of the segment is likely to increase the catalytic efficiency of the Q81L mutant. A similar result was previously reported for MPH from *Ochrobactrum* sp. (Tian *et al*., 2010).

Conclusion

We have demonstrated that the screening system based on phenolics-responsive transcription activator can be effectively used for directed evolution of OP-degrading enzymes. Furthermore, the screening system offers versatility for various OPs with phenolic groups. The utility of the screening system was shown by the successful generation of a mutant with a 100-fold higher k_{cat}/K_m than the wild-type enzyme by directed evolution. More than 50% of widely used OP pesticides as well as synthetic analogues of G-type nerve agents are shown to contain a phenolic group, and this phenolic group is released by OP-degrading enzymes (Pope, 1999; Tsai *et al*., 2010). Such synthetic analogues have been successfully employed for developing the enzymes for nerve agents. Hence, the present screening system can find wide applications in the development of the enzymes for detoxification and decontamination of various OP pesticides and nerve agents.

Supplementary data

Supplementary data are available at *PEDS* online.

Acknowledgement

We thank Y. Han for technical assistance in the use of a FACSAria™ and a full HTS system at KRIBB Jeonbuk branch.

Funding

This research was supported by Dual Use Technology Project (08-DU-EB-01), Advanced Biomass R&D Center (ABC) of Global Frontier Project, Brain Korea 21, Intelligent Synthetic Biology Center (2011-0031951, 2011-0031944) and World Class University program (Grant R31-2010-000-10071) from MEST. The work in KRIBB was supported by grants from KRCF and NRF.

References

Arnold,K., Bordoli,L., Kopp,J. and Schwede,T. (2006) *Bioinformatics*, **22**, 195–201.
Berendsen,H.J.C., Postma,J.P.M., DiNola,A. and Haak,J.R. (1984) *J. Chem. Phys.*, **81**, 3684–3690.
Berendsen,H.J.C., Postma,J.P.M., van Gunsteren,W.F. and Hermans,J. (1981) In Pullman,B. (ed.), *Intermolecular Forces*. D. Reidel Publishing Company, Dordrecht, pp. 331–342.
Briseño-Roa,L., Hill,J., Notman,S., *et al*. (2006) *J. Med. Chem.*, **49**, 246–255.
Chen,Y., Zhang,X., Liu,H., Wang,Y. and Xia,X. (2002) *Acta Microbiol. Sin.*, **42**, 490–497.
Cheng,T.C., Harvey,S.P. and Chen,G.L. (1996) *Appl. Environ. Microbiol.*, **62**, 1636–1641.
Cho,C.M., Mulchandani,A. and Chen,W. (2002) *Appl. Environ. Microbiol.*, **68**, 2026–2030.
DeFrank,J.J. and Cheng,T.C. (1991) *J. Bacteriol.*, **173**, 1938–1943.
DeLano,W.L. (2002) *The PyMOL Molecular Graphics System*. DeLano Scientific, San Carlos. http://pymol.sourceforge.net/.
Di Sioudi,B.D., Miller,C.E., Lai,K., Grimsley,J.K. and Wild,J.R. (1999) *Chem. Biol. Interact.*, **119–120**, 211–223.
Dong,Y.J., Bartlam,M., Sun,L., Zhou,Y.F., Zhang,Z.P., Zhang,C.G., Rao,Z. and Zhang,X.E. (2005) *J. Mol. Biol.*, **353**, 655–663.
Griffiths,A.D. and Tawfik,D.S. (2003) *EMBO J.*, **22**, 24–35.
Guex,N. and Peitsch,M.C. (1997) *Electrophoresis*, **18**, 2714–2723.
Hess,B., Kutzner,C., Van Der Spoel,D. and Lindahl,E. (2008) *J. Chem. Theory Comput.*, **4**, 435–447.
Ibrahim,M.M. and Ramadan,A.M. (2010) *J. Incl. Phenom. Macrocycl. Chem.*, **68**, 287–296.
Krivov,G.G., Shapovalov,M.V. and Dunbrack,R.L., Jr. (2009) *Proteins: Struct. Funct. Bioinf.*, **77**, 778–795.
Menger,F.M. and Tsuno,T. (1989) *J. Am. Chem. Soc.*, **111**, 4903–4907.
Mulbry,W.W., Karns,J.S., Kearney,P.C., Nelson,J.O., McDaniel,C.S. and Wild,J.R. (1986) *Appl. Environ. Microbiol.*, **51**, 926–930.
Murphy,S.D. (1986) In Klaassen,C.D., Amdur,M.O. and Doull,J. (ed.), *Casarett and Doull's Toxicology, The Basic Science of Poisons*. Macmillan Publishing. Co., New York, pp. 519–581.
Omburo,G.A., Kuo,J.M., Mullins,L.S. and Raushel,F.M. (1992) *J. Biol. Chem.*, **267**, 13278–13283.
Oostenbrink,C., Villa,A., Mark,A.E. and van Gunsteren,W.F. (2004) *J. Comput. Chem.*, **25**, 1656–1676.
Pavel,H., Forsman,M. and Shingler,V. (1994) *J. Bacteriol.*, **176**, 7550–7557.
Pope,C.N. (1999) *J. Toxicol. Environ. Health Part B*, **2**, 161–181.
Poo,H.R., Song,J.J., Hong,S.P., Choi,Y.H., Yun,S.W., Kim,J.H., Lee,S.C., Lee,S.G. and Sung,M.H. (2002) *Biotechnol. Lett.*, **24**, 1185–1189.
Schwede,T., Kopp,J., Guex,N. and Peitsch,M.C. (2003) *Nucleic Acids Res.*, **31**, 3381–3385.
Shimazu,M., Mulchandani,A. and Chen,W. (2001) *Biotechnol. Prog.*, **17**, 76–80.
Shingler,V. and Moore,T. (1994) *J. Bacteriol.*, **176**, 1555–1560.
Singh,B.K. and Walker,A. (2006) *FEMS Microbiol. Rev.*, **30**, 428–471.
Tian,J., Wang,P., Gao,S., Chu,X., Wu,N. and Fan,Y. (2010) *FEBS J.*, **277**, 4901–4908.
Tokuriki,N. and Tawfik,D.S. (2009) *Nature*, **459**, 668–673.
Tsai,P.C., Bigley,A., Li,Y., Ghanem,E., Cadieux,C.L., Kasten,S.A., Reeves,T.E., Cerasoli,D.M. and Raushel,F.M. (2010) *Biochemistry*, **49**, 7978–7987.
Van Der Spoel,D., Lindahl,E., Hess,B., Groenhof,G., Mark,A.E. and Berendsen,H.J. (2005) *J. Comput. Chem.*, **26**, 1701–1718.
Vyas,N.K., Nickitenko,A., Rastogi,V.K., Shah,S.S. and Quiocho,F.A. (2010) *Biochemistry*, **49**, 547–559.
Yang,C., Cai,N., Dong,M., Jiang,H., Li,J., Qiao,C., Mulchandani,A. and Chen,W. (2008) *Biotechnol. Bioeng.*, **99**, 30–37.
Yang,H., Carr,P.D., Yu-McLloughlin,S., *et al*. (2003) *Protein, Eng, Des. Sel.*, **16**, 135–145.